

Thermoelectric properties of GaAs-Ga_{1-x}Al_xAs heterojunctions at high magnetic fields

R. Fletcher* and J. C. Maan

Hochfeld Magnetlabor, Max-Planck-Institut für Festkörperforschung, 166X, F-38042 Grenoble Cédex, France

K. Ploog

Max-Planck-Institut für Festkörperforschung D-700 Stuttgart 8, Federal Republic of Germany

G. Weimann

Forschungsinstitut der Deutschen Bundepest, D-6100 Darmstadt, Federal Republic of Germany

(Received 26 December 1985)

Detailed results are presented on both the thermoelectric and resistive coefficients of four high-mobility GaAs-Ga_{1-x}Al_xAs heterojunctions at fields up to 20 T. In the presence of a field both the thermopower and Nernst-Ettingshausen (NE) data behave qualitatively as expected from the predictions of the diffusion model but the magnitudes of both coefficients are always too large; in particular, in the quantum limit at $\nu = \frac{1}{2}$, the thermopower has a magnitude of -50 mV K^{-1} instead of the expected $-120 \mu\text{V K}^{-1}$. The zero-field thermopower is also found to be too large and have the wrong temperature dependence to be ascribed to diffusion. It is possible that phonon drag is responsible for these anomalies though the NE coefficient shows a variation with field which is characteristic of diffusion and it is difficult to reconcile this with phonon drag. The fractional quantum Hall effect (FQHE) is visible in the NE coefficient but not in the thermopower; this makes it possible to trace the sensitivity to the FQHE to a particular component of the thermoelectric tensor.

I. INTRODUCTION

The occurrence of two-dimensional (2D) electron gases in a number of fabricated structures provides a unique opportunity to examine the effects of magnetic quantization on the transport properties. In 3D electron gases, the direction parallel to the magnetic field \mathbf{B} is unquantized by the field and is responsible for a large quasiclassical background on which the effects of quantization are observed. As an example, the quantum oscillations in the transverse resistivity ρ_{xx} of metals are typically at the 1% level and for many purposes are negligible. On the other hand, for a 2D metallic gas with \mathbf{B} perpendicular to the plane, the quantization is complete and oscillations at the 100% level are observed. The resistivity coefficients of these systems (i.e., ρ_{xx} and the Hall resistivity ρ_{yx}) have been studied over a wide range of temperatures and fields; this has led to the important discoveries of the quantum Hall effect¹ (QHE) and the fractional quantum Hall effect (FQHE).²

It is natural to extend these studies to the other transport coefficients, i.e., the thermal and thermoelectric effects. At the present time, the former appear to be beyond experimental reach because the 2D gas has an extremely high thermal resistivity W_{xx} in the presence of \mathbf{B} . If one crudely approximates³ $W_{xx} \sim \rho_{xx}/L_0T$, where L_0 is the Lorenz number ($\pi^2 k^2/3e^2$), and puts $\rho_{xx} \sim 1 \text{ k}\Omega$, then $W_{xx} \sim 10^{10} \text{ K W}^{-1}$ at 4 K, an enormous value which will cause severe experimental difficulties. Thus one is left with only the thermoelectric coefficients, and these form the subject of the present paper. There already exist brief reports of experimental work in this regard. Obloh *et al.*^{4,5} presented data on both the thermopower and

Nernst-Ettingshausen coefficient (see Sec. II for definitions) of GaAs-Ga_{1-x}Al_xAs heterostructures at fields up to about 6 T. They obtained good agreement between the thermopower and theoretical calculations. Nicholas *et al.*⁶ and Vuong *et al.*⁷ have presented thermopower results on Ga_{0.47}In_{0.53}As-InP, Ga_{0.47}In_{0.53}As-Al_{0.48}In_{0.52}As, and GaAs-Ga_{0.7}Al_{0.3}As heterojunctions up to 10 T. The former two gave results much smaller than predicted but the last gave data in good agreement with theory. However, mobilities were not presented in the later work⁷ and so it is difficult to compare these results with those of Obloh *et al.*⁴

The present results were all obtained with GaAs-Ga_{1-x}Al_xAs heterojunctions and each sample has a high mobility ($17.1\text{--}37.7 \text{ m}^2 \text{ V}^{-1} \text{ s}^{-1}$ at 4.2 K). With fields of about 20 T available, it was possible to reach the quantum limit for two of the samples (i.e., the field region where all the electrons are in the last Landau level, with spin splitting completely resolved) and in the case of the highest mobility sample, the FQHE is visible in ρ_{xx} at our lowest available temperature ($\sim 1.7 \text{ K}$). These are clearly interesting regimes in which to study the physical properties of these materials and one hopes that these new measurements will shed more light on the thermoelectric behavior of 2D systems. We find that the experimental coefficients have many common features with the theoretical predictions but, for these high-mobility samples, the magnitudes are much higher than expected. In the extreme case of the quantum limit, we find thermopowers in the region of 50 mV K^{-1} . These are giant values by any standards, and in fact are over 2 orders of magnitude larger than expected. A preliminary report of the results on one of the samples has already appeared.⁸

II. THEORY

The thermopower tensor \vec{S} is defined by the relation $\mathbf{E} = \vec{S} \cdot \nabla T$ where \mathbf{E} is the measured electric field produced by the temperature gradient ∇T . For a 2D system there are only two independent coefficients $S_{xx} = S_{yy}$ and $S_{yx} = -S_{xy}$ which are referred to as the thermopower and Nernst-Ettingshausen coefficient, respectively (the field \mathbf{B} is assumed to be along \hat{z} and is perpendicular to the plane). For calculational purposes, one writes \vec{S} in terms of the fundamental transport tensors defined by $\mathbf{J} = \vec{\sigma} \cdot \mathbf{E} - \vec{\epsilon} \cdot \nabla T$ where $\vec{\sigma}$ is the conductivity and $\vec{\epsilon}$ the thermoelectric tensor, \mathbf{J} being the electric current density. The measurements are made with $\mathbf{J} = 0$ and $\partial T / \partial y = 0$ (this latter assumes that the substrate shows no transverse effects) so that

$$S_{xx} = (\vec{\sigma}^{-1} \cdot \vec{\epsilon})_{xx} = \rho_{xx} \epsilon_{xx} - \rho_{yx} \epsilon_{yx} \quad (1)$$

and

$$S_{yx} = (\vec{\sigma}^{-1} \cdot \vec{\epsilon})_{yx} = \rho_{yx} \epsilon_{xx} + \rho_{xx} \epsilon_{yx}. \quad (2)$$

Here we have used the relationship $\vec{\rho} = \vec{\sigma}^{-1}$, $\vec{\rho}$ being the resistivity.

In general, there are two contributions to $\vec{\epsilon}$, carrier diffusion effects and phonon drag effects. At the present time only the former have been treated in detail⁹⁻¹² though recently attention has been drawn to the latter¹³ for these systems.

In the case of diffusion effects, some insight into the behavior of $\vec{\epsilon}$ can be obtained from the Mott approximation¹⁰ that $\vec{\epsilon} = -(\pi^2 k^2 T / 3e) (\partial \vec{\sigma} / \partial E_F)$ where E_F is the Fermi energy of the electrons and $e = |e|$ is the electronic charge. This relation assumes that $\vec{\sigma}$ is a weak function of E_F on an energy scale of order kT . At high magnetic fields in the disorder-free limit, both ρ_{xx} and ϵ_{xx} are zero so $S_{yx} = 0$ and $S_{xx} = -\rho_{yx} \epsilon_{yx}$. To understand how ϵ_{yx} behaves, one imagines starting with E_F at the bottom of a Landau level and adding electrons. This results in E_F increasing and σ_{yx} increasing (since it is given by $\sigma_{yx} = Ne/B$) but because there are many states at the same energy, E_F increases only slowly. Thus $\partial \sigma_{yx} / \partial E_F$ is large. The coefficient $-\epsilon_{yx}$ increases rapidly until the center of the Landau level is reached by E_F , after which it decreases, becoming zero as the level is filled. E_F now traverses the gap $\hbar\omega_c$ between the levels very rapidly with σ_{yx} unchanged, thus holding ϵ_{yx} at zero. Experimentally, E_F is varied by changing the magnetic field, which results in changes in the degeneracy of the Landau levels.

The same result can be seen from a different point of view. In the same disorder free limit it is found that the thermopower is a direct measure of the entropy of the electrons per unit charge density.¹¹ This result is universally valid and applies equally well to bulk semiconductors and metals, with or without a magnetic field. In the present case the appropriate thermopower is S_{xx} , and $-eS_{xx}$ measures the entropy per electron. As B increases and E_F sweeps through the Landau levels, the entropy reaches maxima for half filled levels and is zero for completely full or empty levels; thus $-eS_{xx}$ oscillates as a function of B . Both viewpoints give numerically similar results,¹⁰ with the latter being exact for no disorder. In

particular, when spin splitting is unresolved, the maxima are given by

$$S_{xx} = - \left(\frac{k}{e} \right) \frac{\ln 2}{(n + \frac{1}{2})}, \quad (3)$$

where n is the quantum number of the level in which the Fermi level lies ($n=0,1,\dots$). If spin splitting is resolved¹⁰ the appropriate equation is

$$S_{xx} = - \left(\frac{k}{e} \right) \frac{\ln 2}{(2n + 1 \pm \frac{1}{2})} = - \left(\frac{k}{e} \right) \frac{\ln 2}{\nu}, \quad (4)$$

where ν is the filling factor, defined as the ratio of the number of electrons to the number of states available in a spin resolved level. Both equations assume $kT \ll \hbar\omega_c$ [and kT is much less than spin splitting in Eq. (4)]. In the quantum limit, i.e., $\nu < 1$, the entropy increases without limit as B increases so that S_{xx} increases monotonically with B ; however, Eqs. (3) and (4) are still appropriate when the level is just half filled and at this point the predicted value for S_{xx} is $-120 \mu\text{V K}^{-1}$. The maximum peak height occurs for the second to last Landau level and should be $-40 \mu\text{V K}^{-1}$ [i.e., $n=1$ in Eq. (3) or $\nu = \frac{3}{2}$ in Eq. (4)].

For moderate disorder, the results for S_{xx} are unchanged (because $\rho_{xx} \ll |\rho_{yx}|$ and $|\epsilon_{xx}| \ll |\epsilon_{yx}|$) but S_{yx} now becomes finite. Calculations suggest^{9,10} that the first term in Eq. (2) is the most important if the disorder is not too high. Since ϵ_{xx} will mirror $\partial \sigma_{xx} / \partial E_F$, we expect S_{yx} to pass through zero when σ_{xx} is a maximum (which closely corresponds to a maximum in ρ_{xx}) and thus we expect to see a negative and positive peak as E_F traverses a Landau level. The detailed calculations predict peak heights to be independent of n , and should be in the region of $10-30 \mu\text{V K}^{-1}$.

Finally, when B is zero the diffusion thermopower $S^d = \epsilon_{xx} / \sigma_{xx}$ is expected to be given by¹³

$$\begin{aligned} S^d &= -(\pi^2 k^2 T / 3e E_F) (p + 1) \\ &= -284(p + 1) \left(\frac{T}{T_F} \right) \mu\text{V K}^{-1}, \end{aligned} \quad (5)$$

where p is a factor determined by the energy dependence of the electronic scattering, expected to be about unity for the present case, and $kT_F = E_F$. Notice that for $p=0$, $-eS^d$ is just equivalent to the entropy per electron as before.

There are no detailed calculations of the phonon drag contribution, though Nicholas¹³ has pointed out that an argument due to Herring¹⁴ can be applied to this situation. Herring calculated the Peltier coefficient Π by considering the momentum transferred from an electric current in the electron gas to the phonon current, which in turn implies a heat flux. The thermopower is then obtained from the Kelvin-Onsager result $S = \Pi / T$. The result, for zero B , is

$$S^g = - \frac{f \Lambda v}{\mu T}, \quad (6)$$

where Λ and v are the phonon mean-free path and velocity

TABLE I. Various useful parameters for the samples. N is the electron density, μ the mobility, l_x the length between the contacts used to determine S_{xx} , ν the filling factor and T_F the Fermi temperature (assuming the effective mass $m^* = 0.066m_e$).

Sample number	$N(10^{15} \text{ m}^{-2})$ $\pm 2\%$	$\mu(4.2\text{K})$ ($\text{m}^2 \text{V}^{-1} \text{s}^{-1}$) $\pm 5\%$	Overall dimensions (mm^3)	$\nu=1$ at $B(T)$	l_x (mm)	T_F (K)
1	1.78	22.6	$5 \times 10 \times 0.36$	7.36	0.98	75
2	4.80	37.7	$6 \times 12 \times 0.44$	19.8	0.63	202
3	6.82	24.9	$6 \times 12 \times 0.41$	28.2	2.98	287
4	2.35	17.1	$3 \times 9 \times 0.48$	9.72	0.97	99

ty, μ is the mobility of the electrons, and f an efficiency factor which represents that fraction of the electron momentum which is given to the phonons. This last term can be approximated as $f = \mu/\mu_p$ where μ_p is the mobility that the electrons would have if only phonon scattering were present. In the boundary scattering limit, which is appropriate to pure single crystals at low temperatures, Λ is determined by the sample dimensions and would be ~ 0.8 mm for the present samples. With $\mu_p \sim 3000/T \text{ m}^2 \text{V}^{-1} \text{s}^{-1}$ and $\nu \sim 4000 \text{ m s}^{-1}$, then $S^g \sim -1 \text{ mV K}^{-1}$. At helium temperatures this is much larger than S^d , even for a Fermi temperature T_F as low as 100 K.

As the temperature is increased, other phonon scattering mechanisms (e.g., phonon-phonon or phonon-isotope) will serve to decrease Λ and cause $-S^g$ to decrease. At low temperatures, the situation is not clear but Nicholas¹³ has suggested that $-S^g$ will decrease because μ_p rises faster than that given by the relationship above. Another possibility will be mentioned in Sec. IV.

Nicholas¹³ has attempted to extend the above analysis to high fields, but the argument is not convincing. Nevertheless, in view of the large effects that seem to be possible at zero field, it does seem likely that phonon drag will be important at high fields.

III. EXPERIMENTAL TECHNIQUES AND RESULTS

The heterojunctions were grown on GaAs substrates by molecular-beam epitaxy; the dimensions of the substrates and some further information are given in Table I. Selective etching produced 2D samples of standard shape suitable for the measurement of the electrical resistivities ρ_{xx} and ρ_{yx} ; these 2D samples had overall dimensions of about $1.3 \times 3.0 \text{ mm}^2$. Ten Sn contacts were diffused into the surface, the final diameters being about 0.3 mm, and to these contacts were In soldered 5 mm lengths of 50- μm diam annealed Cu wire. Each sample was mounted above a glass filled epoxy disc, being supported at the cold-sink end only (Fig. 1). Ten lengths of 100- μm diam Manganin wire were threaded through small holes in the disc, and soldered to copper contacts on the disc so as to leave about 10 mm of wire on the sample side. These, in turn, were soldered to the 50- μm Cu wires from the sample. In this way, there was no appreciable heat leak from the sample (each 10-mm Manganin wire having a thermal resistance of $\sim 5 \times 10^5 \text{ K W}^{-1}$ at 10 K). Because the copper wires remain isothermal and thus play no part in

the thermoelectric voltage, the experiments determine the thermopower between the sample and Manganin, this latter contributing very little since it has a thermopower of $< 1 \mu\text{V K}^{-1}$ over the temperature range of interest.¹⁵

Voltages were measured using a Keithley 155 microvoltmeter with a noise and drift $\sim 0.1 \mu\text{V}$ and an offset current of $\leq 20 \text{ pA}$. Because the input impedance is only $1 \text{ M}\Omega$ and the output impedances of the samples are typically 30–40 $\text{K}\Omega$ at 20 T, the effective gain of the instrument is reduced by 3–4% at high fields. Corrections were not made for this effect.

In the measurement of the thermopower, it is important to realize that the effective length of the sample is not determined by the separation of the limbs, as would be the

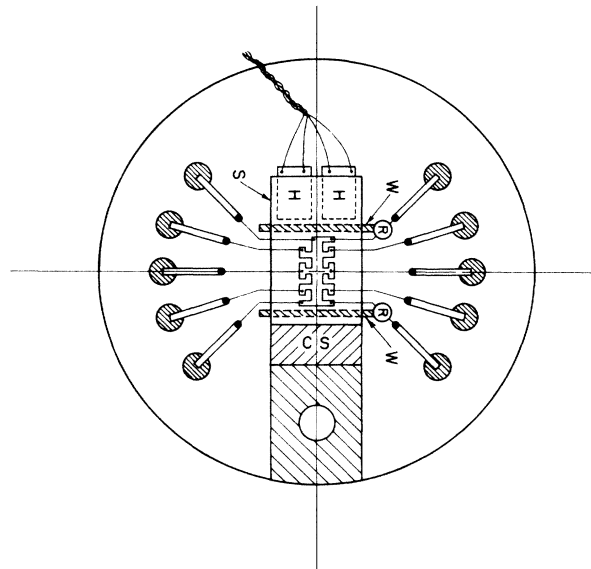


FIG. 1. Sample mounting. The sample S is attached to the cold sink CS and heaters H by Ag paint. The carbon resistors R are soldered to 200 μ diam Cu wires W which in turn are epoxied to the sample. Electrical contacts to the sample are made with 50- μ diam annealed Cu wires which are soldered to 100- μ diam Manganin wires; these, in turn, are soldered to the circular glass filled epoxy circuit board below the sample. The heat sink is also soldered to the circuit board. The figure is drawn approximately to scale, the circular board being 24 mm diam.

case for ρ_{xx} . The relevant length is that between the Sn contacts themselves, because the temperature gradient extends over the complete sample, including the limbs. The lengths appropriate to S_{xx} are given in Table I under the column l_x . It will be seen that the diameter of the tin contacts, at 0.3 mm, is comparable to l_x , and this provides the largest source of uncertainty in these experiments, being about 10% in the best case of sample 3 and 50% in the worst case of sample 2. (One naturally attempts to find pairs of contacts with the largest separation, but not all contacts are usable, especially at high fields where the resistance of some contacts is very large.) In the case of S_{yx} all contact pairs are between 1–1.3 mm apart, giving a constant error of about 25%. These uncertainties generally dominate the final absolute accuracy of the thermoelectric data.

Thermally bonding the sample to the cold sink and heaters proved to be a more difficult problem than expected. Initially, General Electric 7031 varnish and silver filled epoxy were tried, but these regularly damaged the samples on thermal cycling, usually by pulling off the surfaces. These effects are clearly caused by differential thermal expansion, the expansion coefficient of GaAs being very low¹⁶ at $\sim 5.5 \times 10^{-6} \text{ K}^{-1}$ at 300 K (which is approximately one third that of copper). Finally, Ag paint was used and in spite of its low strength, most bonds survived cooldown, sometimes repeatedly, and in no case was damage ever observed on the sample surfaces. Regardless of the bonding material (epoxy, varnish, or Ag paint) the thermal resistances of the bonds were very similar and an order of magnitude larger than one would estimate from the known thermal conductivities of the bonding materials. Tests made with Cu-Cu joints gave no such discrepancy and we conclude that the difficulty with GaAs is caused by the thermal boundary (or Kapitza) resistance.¹⁷

The heater consisted of a pair of Constantan strain gauges (each of active area $1.0 \times 1.5 \text{ mm}$ and 350- Ω resistance) mounted side by side to help produce a uniform temperature gradient (Fig. 1). These gauges had the useful feature of allowing the whole system to achieve a very rapid equilibrium time but they were found to have a negative magnetoresistance amounting to about 10% at 20 T. This feature was actually quite useful because the sample temperature inevitably increased with field, perhaps because of the thermal magnetoresistance of the copper, which carries the heat to the liquid helium; by using a constant current generator to drive the heaters, the dissipated power decreased with field and tended to offset the temperature rise. Even so, there was always a temperature increase whose magnitude depended on the temperature and the sample; at the lowest temperature the effect never exceeded 0.1 K, but it varied between 0.2 and 1 K for the different samples at the highest temperatures, with the lower values being the most common.

Temperature gradients were determined by matched pairs of 220- Ω $\frac{1}{8}$ -W carbon resistors mounted on the samples by the following technique. Short lengths of 200- μm diam Cu wires were flattened to an approximately rectangular shape ($0.1 \times 0.3 \text{ mm}^2$). Each carbon resistor was soft soldered to one end of such a wire, which in turn was

bonded across the underneath of the GaAs plate using the minimum possible amount of epoxy cement (Ag paint having too little strength). This arrangement caused no observable damage to the samples on cooldown. A pair of 50- μm diam Manganin leads, with a minimum free length of about 20 mm, was used to provide electrical connections to each resistor. The thermal resistance of such a pair is estimated to be $\sim 10^6 \text{ K W}^{-1}$ at 10 K, compared to that of the epoxy joint at 2000 K W^{-1} (which includes the observed thermal boundary resistance referred to above). Hence, for a sample at a temperature 5 K higher than the cold sink, the maximum allowed in these experiments, there will be a temperature difference of perhaps 10 mK between each thermometer and the sample. However, because each thermometer of the pair is at a very similar temperature, these errors should be essentially identical and cancel when taking the temperature difference; it is difficult to see how errors of more than a few percent could arise from this source. The resistors themselves were driven by a constant voltage bridge and dissipated a few nW at 4.2 K; this has a negligible effect on their temperatures. The resistors were calibrated on every run using a commercial Ge thermometer which was embedded in the cold sink. With the standard heat leak to the bath, the cold sink could be heated to about 9 K and all of the high-field data were taken with the cold sink in the range 1.4–9 K. However, by reducing the heat leak to the bath, temperatures of at least 30 K were possible and thermopower data at zero field was usually taken up to this temperature. Above 30 K, the 220- Ω carbon resistors become too insensitive to be useful as thermometers. Because the temperature of the cold sink was controlled using a capacitance thermometer as the sensing element, we were able to calibrate the resistors as a function of field as well as temperature. This was done by setting a specific temperature at zero field (measured with the Ge thermometer) and using the capacitance controller to hold the temperature stable while increasing the field.

In order to check the thermometry, sample 1 also had a thermocouple attached to two extra Sn contacts which had been diffused into the GaAs outside the active sample area. This thermocouple was made of a 25-mm length of 0.08-mm diam Au + 0.03 at. % Fe wire plus two long lengths of 0.05-mm diam Manganin, this latter being used in place of the traditional Chromel because it was of smaller diameter and more flexible. In the low-temperature range we anticipate little difference in sensitivity will be incurred by the use of Manganin rather than Chromel. The gradients as measured by the two techniques for $4 < T < 20 \text{ K}$ agreed to $\leq 6\%$, which is taken as a satisfactory check on the thermometry in view of the different active lengths and the uncertainty in the precise sensitivity of the thermocouple. (The length of GaAs over which the temperature gradient was measured was between 3.5 and 5 mm for the various samples so that with a probe width of 0.3 mm we would expect an uncertainty of up to 10% from this source.) Thermocouples are not useful at high fields and so this check was possible only at zero field.

Because the thermal equilibrium time of the sample and heater were so fast, we attempted to use an ac technique

with sample 1. By driving the heater with a sinusoidal current, (~ 5 Hz) and detecting the output with a lock-in amplifier tuned to twice the frequency, good signal-to-noise was possible. Unfortunately, it appeared that small changes in the thermal resistance at the heater and cold sink occurred on successive cooldowns which changed the calibration factors from day to day. On an initial run this technique gave data in good agreement with dc data but it was abandoned because of calibration problems.

Magnetic fields were usually provided by a 10-MW Bitter-Style magnet capable of 20 T in a 50-mm bore. Some data were taken at fields up to 23 T using a polyhelix magnet with the same bore. There is little hysteresis with water-cooled magnets so the current gives an

accurate measure of the magnetic field.

To unravel the various contributions to S_{xx} and S_{yx} [cf. Eqs. (1) and (2)], one also needs data on ρ_{xx} and ρ_{yx} at the same temperature. Thus data on all these coefficients were obtained at each of 3–4 temperatures between 1.7 and 9.0 K. This entailed making a field sweep for each direction of \mathbf{B} , and in the case of S_{xx} and S_{yx} , zero temperature gradient sweeps were also required to enable any base line corrections to be made. In all cases the temperature was controlled so that all the data were taken at the same fixed temperature, as far as possible. The resistivity data were analyzed simply by taking differences or sums

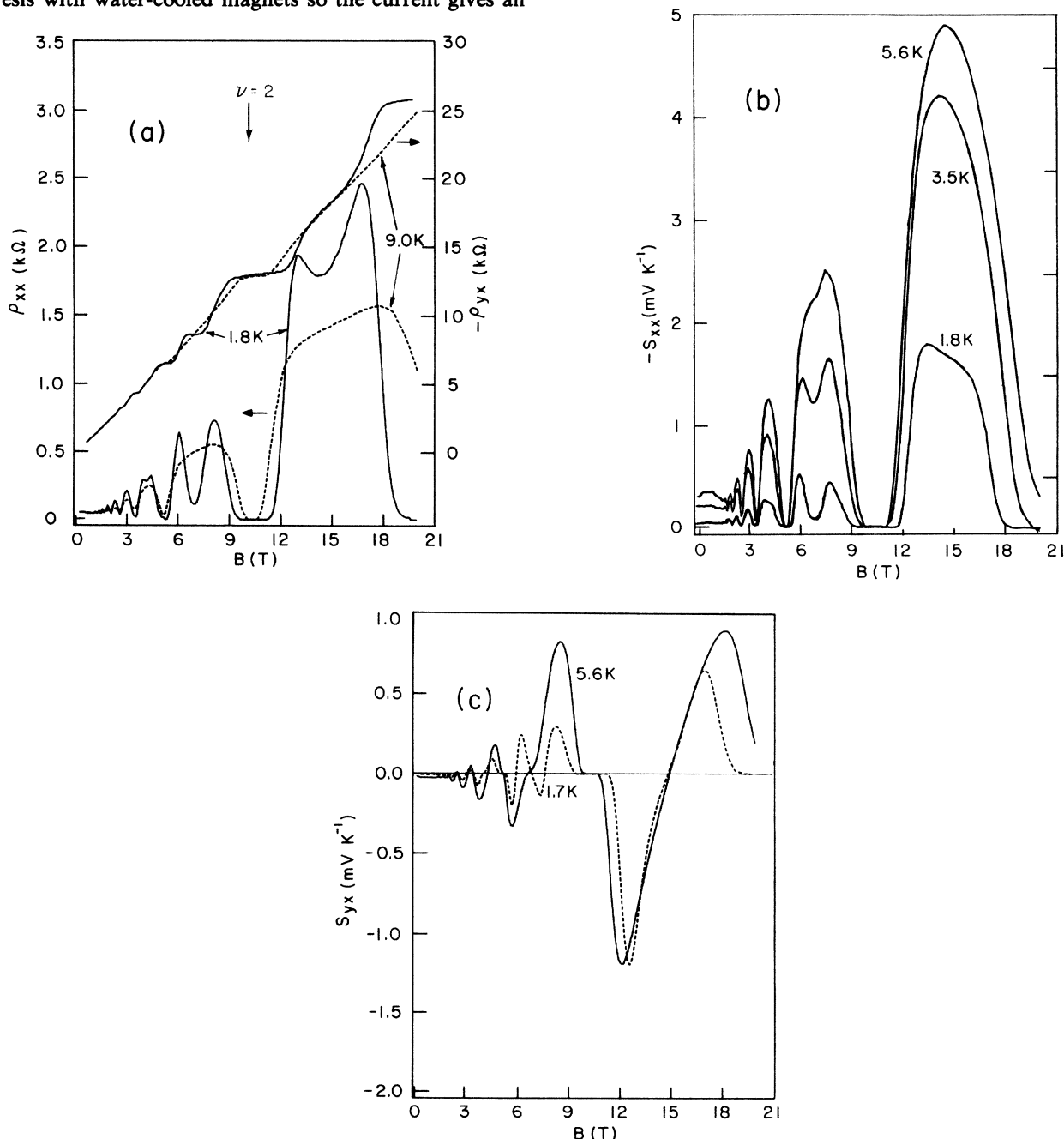


FIG. 2. Experimental data for sample 2. (a) ρ_{xx} and $-\rho_{yx}$, (b) $-S_{xx}$, and (c) S_{yx} .

of the $\pm B$ data as is appropriate to the symmetry of the coefficients. In the case of ρ_{yx} there were no significant differences between $\pm B$ sweeps apart from the sign, whereas for ρ_{xx} the differences varied from sample to sample and were $\leq 10\%$. The same procedures were followed for the thermoelectric coefficients except where there were significant base line effects which were subtracted first. S_{xx} and S_{yx} were quite close to being purely symmetric and antisymmetric in B respectively, though $\pm B$ sweeps were essential in removing any admixture of the unwanted component, particularly for S_{yx} .

Sets of data on ρ_{xx} , ρ_{yx} , S_{xx} , and S_{yx} are shown in Figs. 2–4 (see also Ref. 8 for more information on sample 1). For the sake of clarity some data have been omitted at low B . We find that the thermoelectric coefficients are relatively insensitive to T in the range of 5–9 K and so only a single data set is shown for each sample in this region. Figure 5 illustrates this feature for S_{xx} by showing the magnitude as a function of T for samples 1 and 3 at various fields. Finally, Figs. 6(a) and 6(b) show zero-field results on S [i.e., $S_{xx}(B=0)$]. The data for sample 4 are limited to below 10 K because on this sample the thermal

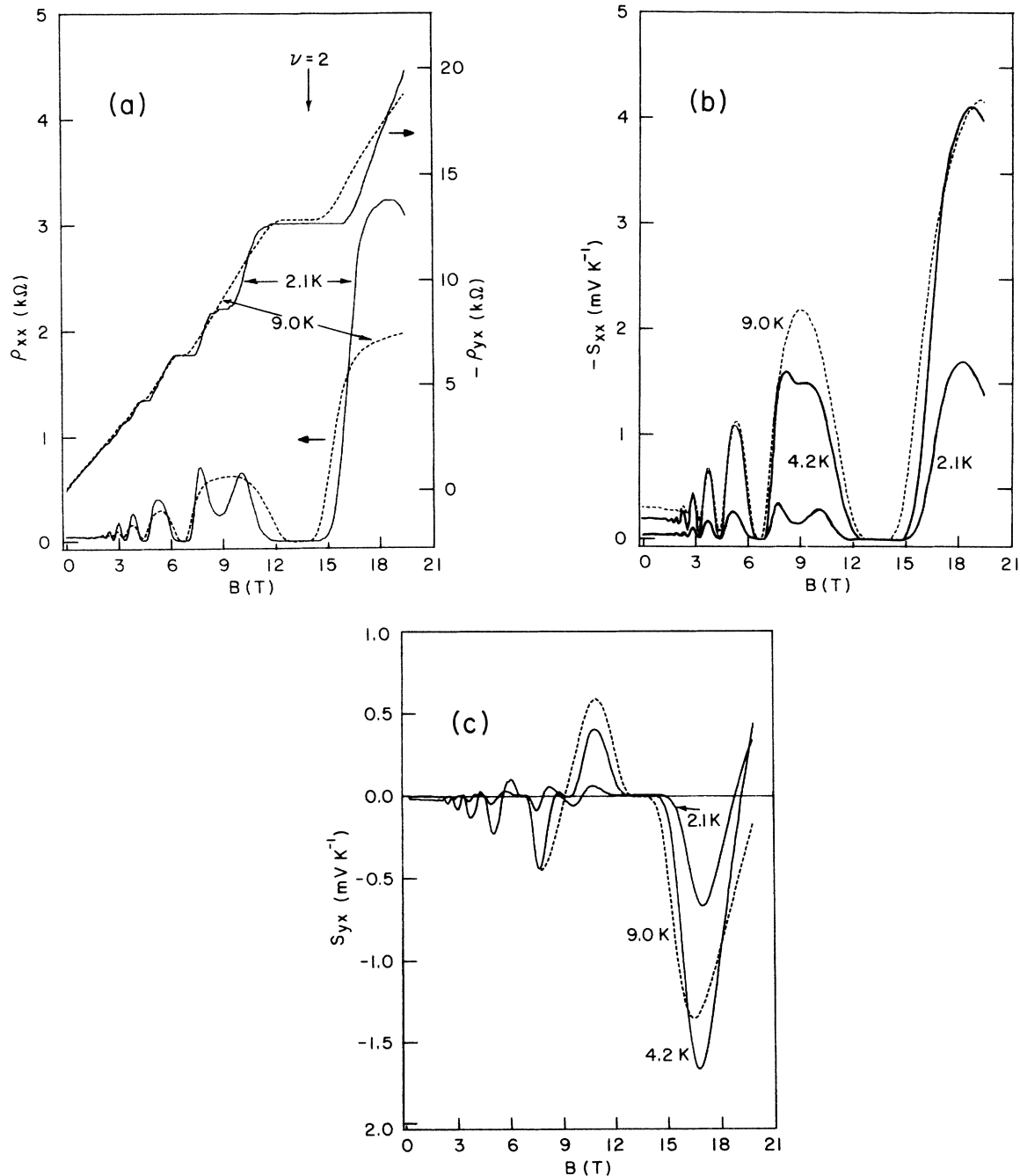


FIG. 3. Experimental data for sample 3. (a) ρ_{xx} and $-\rho_{yx}$, (b) $-S_{xx}$, and (c) S_{yx} . For clarity the data for 9.0 K are suppressed below 7 T but they are very similar to those at 4.2 K at low B .

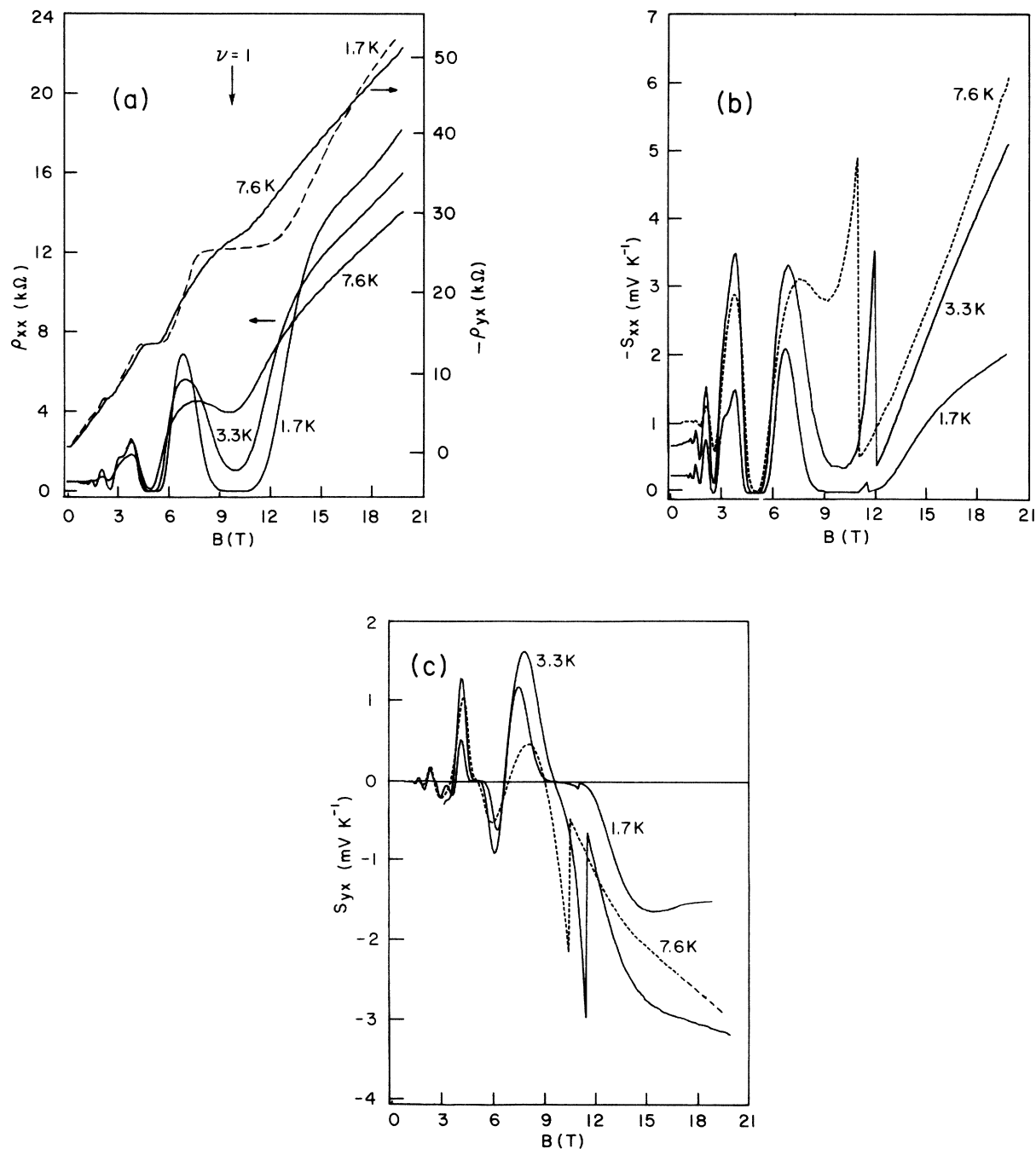


FIG. 4. Experimental data for sample 4. (a) ρ_{xx} and $-\rho_{yx}$. For clarity the data on ρ_{xx} at 3.3 K are suppressed below 3.5 T. ρ_{yx} is relatively T independent and so only one data set is shown. (b) $-S_{xx}$. The discontinuities between 11 and 12 T correspond to scale changes of times 10. (c) S_{yx} . For clarity the data for 3.3 K are suppressed below 3.5 T. Notice the scale changes of times 5 near 12 T.

bonds failed when the cryostat was warmed to room temperature to change the heat leak to the helium bath.

IV. ANALYSIS AND DISCUSSION

From the period of the oscillations as a function of B^{-1} , one can evaluate the electron density in each of the samples. This information is shown in Table I together

with the mobilities as determined from the zero-field values of ρ_{xx} .

It became evident in analyzing the results that sample 4 was often significantly different from the other three samples. This seems to arise from the fact that the latter were grown on Cr-doped substrates while the former was grown on a semi-insulating substrate. The difference is most pronounced in the thermal conductivities of the sub-

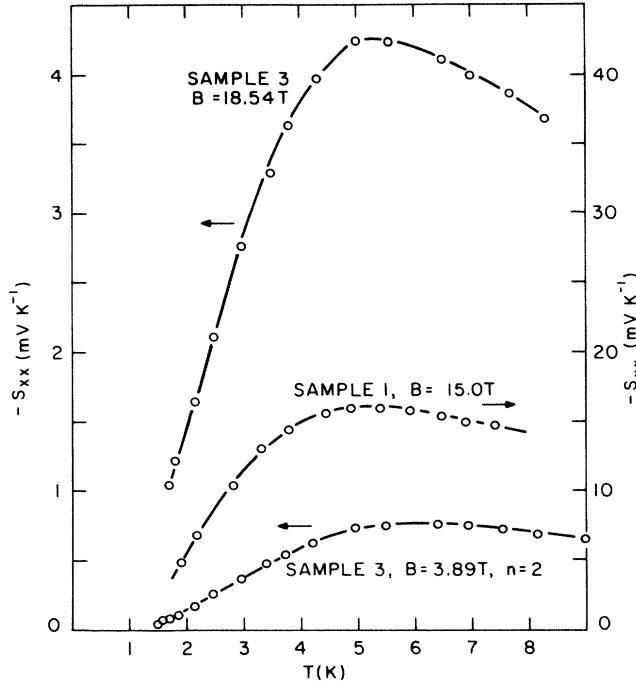


FIG. 5. Some data on the magnitude of $-S_{xx}$ for samples 1 and 3 at various fixed B as a function of T . For sample 3, the data at 18.54 T correspond to $\nu = \frac{3}{2}$ and those at 3.89 T to $n=2$ [cf. Fig. 3(b)]. In the case of sample 1, the data correspond to $\nu = \frac{1}{2}$. The data for other samples at various B show a similar variation with T .

strates which will be presented before proceeding to an analysis of the thermoelectric data. Since one measures thermopower and thermal conductivity λ under identical adiabatic conditions, one need only measure the heater power to extract λ . The results are shown in Fig. 7. It is clear that samples 1–3 have essentially the same λ , bearing in mind an absolute uncertainty of about 10% for each data set, whereas that for sample 4 is considerably higher.

The thermal conductivity of pure dielectric crystals is usually determined by boundary scattering at low temperatures. Under these conditions, λ is given by¹⁸

$$\lambda = \frac{2\pi^2}{15} \frac{k\Lambda}{v^2} \left[\frac{kT}{h} \right]^3, \quad (7)$$

where Λ is the phonon mean-free path and v the sound velocity (given by $1/v = 1/3[(2/v_t) + (1/v_l)]$ with v_t and v_l being appropriate to transverse and longitudinal waves). There appears to be no available calculation for estimating Λ in the case of thin plates, but taking Ziman's calculations for the mean-free path of thin-film conductors as a guide,¹⁹ we anticipate $\Lambda \sim (3/4)t \ln(w/t)$ for the case of $w \gg t$ with w the width and t the thickness of the plates. This produces estimates of Λ at 0.71, 0.86, 0.82, and 0.66 mm (± 10 –20%) for samples 1–4, respectively. Inserting the measured conductivities at ~ 3 K into Eq.

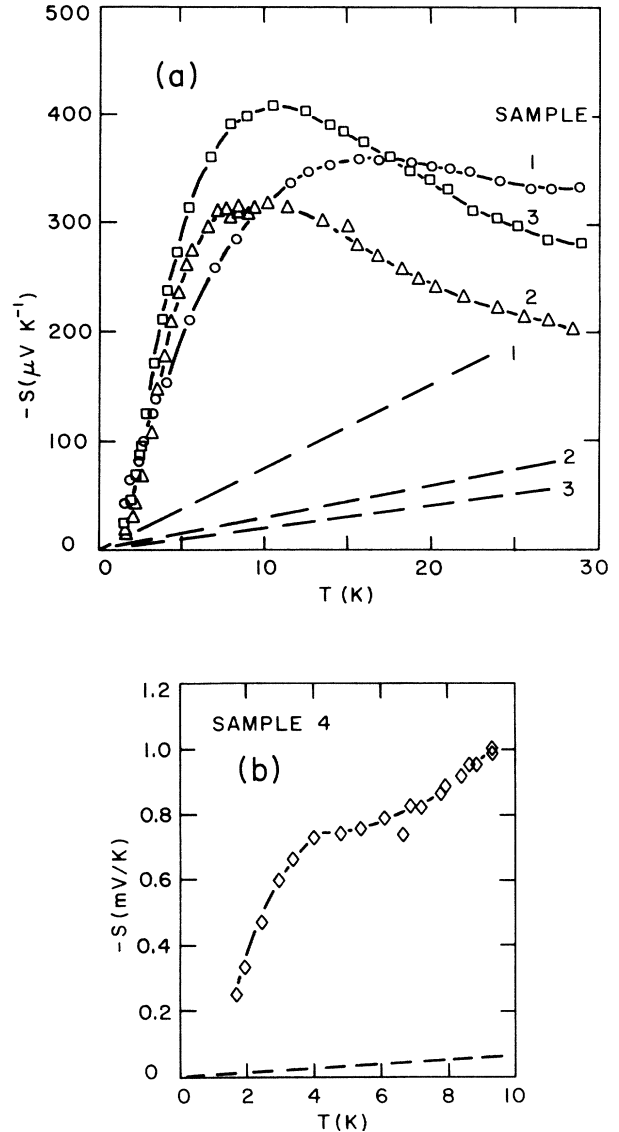


FIG. 6. The zero field thermopower $-S$ as a function of T . The straight lines through the origin are estimates of the diffusion components S^d according to Eq. (5). (a) Samples 1, 2, and 3. (b) Sample 4.

(7) gives measured values of Λ at 0.30, 0.35, 0.41, and 1.4 mm for samples 1–4 (all $\pm \sim 15\%$). The fact that sample 4 gives a measured Λ larger than that expected from the sample dimensions might imply that the epitaxial layer acts as a specular reflector for phonons though electron-phonon scattering in this region must make this imperfect. In any case, it seems clear that the Cr doping in samples 1–3 causes appreciable phonon scattering and reduces Λ by perhaps a factor of 3–4, compared to that of sample 4. The effect of the impurities is consistent with earlier results²⁰ which showed that surprisingly small amounts can severely reduce λ in this temperature range, though why λ should retain the characteristic T^3 dependence of boundary scattering is not clear.

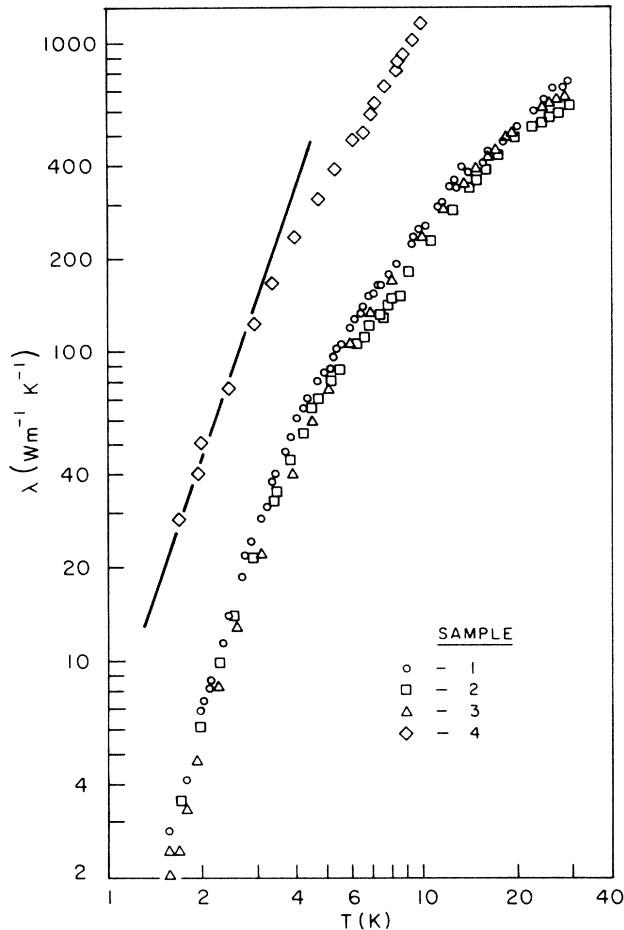


FIG. 7. The thermal conductivity λ for all the samples. The line through sample 4 represents a T^3 variation as would be expected for boundary scattering at low temperatures.

The rapid variation of λ with T has experimental ramifications. As the magnetic field was applied, T invariably increased and even though this was a rather small effect (Sec. III) it resulted in a relatively rapid decrease in the temperature gradient. Such changes were often 20–30% by 20 T. However, in calculating λ from the data we find that it is independent of B for our samples. This is a useful check on the calibration procedures for the carbon thermometers when subjected to high fields.

With regard to both S_{xx} and S_{yx} , it is seen that both coefficients behave qualitatively as expected from the predictions of the diffusion model, discussed in Sec. II, though the absolute magnitudes are completely different. S_{xx} shows peaks which resemble ρ_{xx} in their field dependence; their amplitudes increase roughly in accord with Eqs. (3) and (4), with some notable exceptions to be mentioned shortly. Spin splitting is observed with about the same resolution in both S_{xx} and ρ_{xx} . In both of these coefficients, spin splitting is completely resolved for $n=0$, and partially resolved for $n=1$, depending on B and T . (The fields at which the filling factor $\nu=1$ are shown in

Table I; this enables the peaks in all the figures to be identified with the various Landau levels.) S_{yx} has the expected sign change when the Landau levels are half filled and generally resembles the results of the model calculations. Spin splitting is always better resolved in this coefficient than in S_{xx} or ρ_{xx} ; this is consistent with S_{yx} resembling the derivative of σ_{xx} (cf. Sec. II). In some cases (e.g., sample 2 near 7 T) the increased resolution at low T results in an extra oscillation occurring in S_{yx} (cf. Ref. 5).

This generally good qualitative agreement is offset by large discrepancies with regard to the absolute magnitudes. In the case of S_{xx} , Eqs. (3) and (4) predict a maximum peak height of $-40 \mu\text{V K}^{-1}$ which should be appropriate to both the spin resolved case with $\nu=\frac{3}{2}$, and the spin unresolved case with $n=1$. That the heights of these two peaks should be the same is borne out by samples 1 and 4, but is not the case for samples 2 and 3. Furthermore, we find for samples 2, 3, and 4 ($T \geq 4.5$ K) that $S_{xx} \sim -4 \text{ mV K}^{-1}$ at $\nu=\frac{3}{2}$, which is 2 orders of magnitude larger than expected (sample 1 has $S_{xx} \sim -0.8 \text{ mV K}^{-1}$). In the quantum limit ($\nu < 1$) the discrepancies are even worse. We expect $S_{xx} = -120 \mu\text{V K}^{-1}$ at $\nu=\frac{1}{2}$ but samples 1 and 4 both give about 50 mV K^{-1} (for $T \geq 4.5$ K), a difference of a factor of 400. As the temperature is decreased below 4.5 K, all the experimental values rapidly decrease but we never approach the predicted results in the range of temperature accessible to us. It should be obvious that the differences are completely outside experimental error. This is borne out by the very magnitude of the discrepancies but, in addition, to obtain results consistent with calculations would require that unphysical temperature gradients be present, e.g., the required temperature gradients would often be such that the temperature differences across the samples exceed the maximum temperature of the sample, often by large factors. The many internal checks and consistencies among the data preclude such possibilities. In the case of S_{yx} , the discrepancies are still large but not as startling. The peak heights (both plus and minus) were expected^{9,10} to be about $10\text{--}30 \mu\text{V K}^{-1}$, but experimentally are in the range of $0.1\text{--}1 \text{ mV K}^{-1}$, i.e., perhaps an order of magnitude too large in general.

Before leaving this general survey of the data, we draw attention to the fact that sample 1 shows⁸ the presence of the FQHE in all of ρ_{xx} , S_{yx} , and ρ_{yx} (the last, not presented in Ref. 8, shows a weak plateau near 21 T); this is clearest at $\nu=\frac{1}{3}$ (near 21 T) but is also evident to a smaller extent at $\nu=\frac{2}{3}$ in ρ_{xx} and S_{yx} . From an experimental point of view, it is very surprising that S_{xx} shows no trace of the FQHE under the same conditions of temperature and field. We will return to this aspect later.

The contributions made by each term in Eqs. (1) and (2) may be readily evaluated since we have complete data sets on S and ρ at various temperatures. We find that S_{xx} is almost precisely equal to $-\rho_{yx}\epsilon_{yx}$ under all conditions, any differences never exceeding 5%. This is consistent with the diffusion theory outlined in Sec. II even though the experimental magnitudes are not in agreement. S_{yx} is not completely dominated by either $\rho_{yx}\epsilon_{xx}$ or $\rho_{xx}\epsilon_{yx}$ but the former is usually the most important, especially for $\nu > 1$. Thus there is no doubt that ϵ_{xx} is responsible for

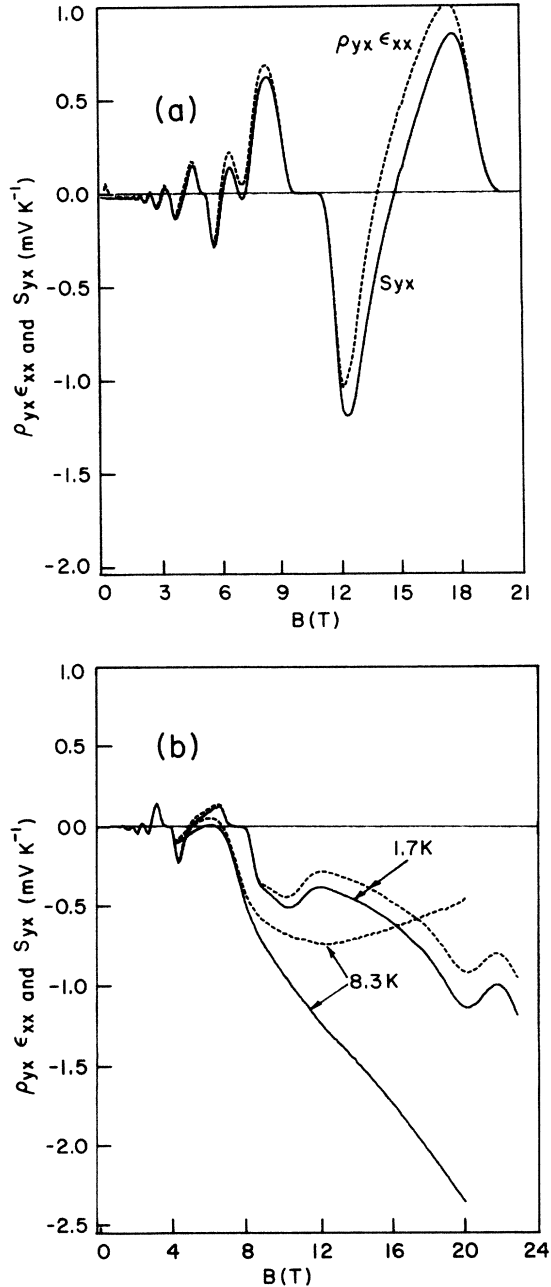


FIG. 8(a) S_{yx} (solid line) and $\rho_{yx}\epsilon_{xx}$ (dashed line) for sample 2 at 3.5 K. (b) S_{yx} (solid line) and $\rho_{yx}\epsilon_{xx}$ (dashed line) for sample 1 at 1.7 and 8.3 K. Only data on S_{yx} at 1.7 K are shown below 4 T, the others being omitted for clarity. However, S_{yx} is closely equal to $\rho_{yx}\epsilon_{xx}$ below 4 T.

the sign changes at half filled Landau levels, and to a large extent for the amplitude of the peaks. To illustrate these features, Fig. 8(a) shows an example of the results for sample 2 and Fig. 8(b) shows similar results for sample 1.

Several conclusions can be drawn from these results.

(i) $\rho_{yx}\epsilon_{xx}$ shows a tendency to saturate for $\nu < 1$ in

agreement with the diffusion model. (This is also true for sample 4 for which data are not shown.)

(ii) Figure 8(b) makes it quite clear that ϵ_{xx} is responding to the FQHE and is primarily responsible for the dip in S_{yx} at $\nu = \frac{1}{3}$. This is contrary to our previous comments⁸ which were made before this analysis was available, i.e., the dip is not simply a consequence of ρ_{xx} via the term $\rho_{xx}\epsilon_{yx}$ and in fact only a relatively small fraction can be ascribed to this source. Notice that if it were still true that ϵ_{xx} behaves like $\partial\sigma_{xx}/\partial E_F$, then one might not have expected a simple dip in S_{yx} , but rather a negative dip followed by a positive peak.

(iii) It is also implicit from our comments above that ϵ_{yx} is insensitive to the FQHE; this follows because $S_{xx} = -\rho_{yx}\epsilon_{yx}$ to high precision, and S_{xx} does not indicate the FQHE.

We will now examine the possibility that some of the discrepancies between theory and experiment are caused by phonon drag. Equation (6) predicts that the temperature variation of S^g will be mainly determined by Λ the phonon mean-free path. The results on Fig. 7 show a variation of λ close to T^3 at $T \leq 3.5$ K for all samples. The decrease of λ below T^3 at higher T is likely caused primarily by the decrease of the specific heat of GaAs below T^3 , and although we expect other scattering mechanisms to reduce Λ at higher T , this is probably a weak effect below ~ 10 K. Hence we anticipated that $-S^g$ would be roughly constant in magnitude with a gentle decline at higher T . The rapid decrease in $-S$ (and hence also $-S^g$) that is observed below ~ 5 K was not expected. We note that Obloh *et al.*⁵ have also seen similar behavior for high-mobility GaAs heterojunctions. Nicholas¹³ has suggested that μ_p will rise faster than the assumed $3000/T \text{ m}^2 \text{ V}^{-1} \text{ s}^{-1}$ as the phonon wave vectors become smaller than the Fermi radius. One might also expect the rapid falloff in the phonon population to be a significant factor at low temperatures, but detailed calculations²¹ suggest that both of these effects must be relatively weak down to 2–3 K. Another possibility is that the phonon drag contribution is saturating in the manner outlined by Herring.¹⁴ If the transfer of momentum between the electron and phonon systems is large enough, then each system is perturbed from equilibrium in a way which inhibits further momentum transfer. This has also been discussed in some detail by Klemens.²² Whether this is the appropriate mechanism for the present case will probably not be clear until detailed calculations become available. In spite of the disagreement between the observed and predicted low T behavior, one can hope to use the measured Λ in Eq. (6) to estimate $-S^g$ in the region of 5–10 K, assuming that our estimates of Λ are still appropriate to this range of T . Doing this yields values of $-S^g$ at 225, 260, 310, and 975 $\mu\text{V K}^{-1}$ for samples 1–4, respectively. The observed $-S^g = -(S - S^d)$ in Figs. 6(a) and 6(b) are consistent with these estimates, and in particular show the much higher value for sample 4.

The above arguments suggest that the experimental results on S may well be consistent with phonon drag, but in the presence of a magnetic field we have little guidance on what to expect. Experimentally, the variation of S_{xx} with T [Figs. 5(a) and 5(b)] is very similar to the variation

of S with T indicating a possible connection. On the other hand, it is very difficult to understand how phonon drag in S_{yx} could mimic the unusual field dependence of this coefficient. On the diffusion model this arises quite naturally from the behavior of $\partial\sigma_{xx}/\partial E_F$ which is responsible for ϵ_{xx} . Indeed, S_{yx} shows all the expected characteristics of the diffusion model (including the saturation at $\nu < 1$ if the contribution from $\rho_{xx}\epsilon_{yx}$ is subtracted) except that the magnitude is too large. From this evidence, one might conclude that S_{yx} is, in fact, not sensitive to phonon drag. That S_{xx} might include a phonon drag contribution, and S_{yx} not, is not as unlikely as it might seem at first sight. If one evaluates Eqs. (1) and (2) for free electron *bulk* metals (ignoring the effects of quantization) then one finds²³ that the phonon drag contribution to S_{xx} is independent of B , whereas that for S_{yx} decreases as B^{-1} at high fields. Herring's argument¹⁴ can also be extended under the same conditions (i.e., no quantization) and yields the same results. However, the effects of quantization are so pervasive in 2D systems that these results may not be relevant to this situation. If they were, the following conclusions would follow.

(1) There would remain a large discrepancy in magnitude between the calculated and experimental S_{yx} .

(2) The fact that S_{xx} is insensitive to the FQHE whereas S_{yx} shows no sensitivity could reflect the fact that S_{yx} is primarily a diffusion effect monitoring $\partial\epsilon_{xx}/\partial E_F$ whereas S_{xx} is primarily phonon drag; notice that Eq. (6) is independent of the number of electrons, and if some condense into a new state separated by an energy gap, this may not immediately reflect itself in the phonon drag contribution.

Until more theoretical information becomes available, the above should be treated as speculation. In general, we are unable to draw any firm conclusions concerning the presence, or otherwise, of phonon drag in the thermoelectric coefficients though we expect further theoretical work to be considerable help in this respect.

V. SUMMARY AND CONCLUSIONS

The thermoelectric coefficients of all the samples exhibit a behavior which is generally consistent with the predictions of the diffusion models, except for the fact that the observed magnitudes are always larger than expected. The NE coefficient, in particular, has the characteristic variation with field that appears to be the signature of diffusion effects, though the observed magnitudes are about an order of magnitude larger than predicted. Because of the contrast between the good qualitative agreement yet poor quantitative agreement, it has been difficult to decide

whether the observed coefficients in a magnetic field are augmented by phonon drag. This is aggravated by the lack of theoretical work in this respect and it is unlikely that firm conclusions will be possible before theoretical guidance becomes available. On the other hand, the zero-field thermopower seems a likely candidate for phonon drag since both the temperature dependence and absolute magnitude cannot be reasonably ascribed to diffusion effects. Nevertheless, more theoretical input is required in order to understand the detailed variation with temperature. Should phonon drag be confirmed, it will likely also affect the phonon-limited resistivity. The mobility in the absence of disorder scattering will be higher than calculations predict²¹ because of mutual dragging which will make phonon-electron scattering less effective.

From an experimental point of view it would be of interest to pursue the thermoelectric measurements to lower temperatures since the coefficients (particularly S_{xx}) are found to be strong functions of temperature below 4 K. Obloh *et al.*⁵ have interpreted their temperature dependence of S_{xx} to the finite width of the Landau levels, but such an approach is clearly incorrect in the present case because of the lack of agreement with the diffusion model on which the analysis is based. More information on the FQHE and its effect on both S_{xx} and S_{yx} at lower temperatures might throw light on why the former is insensitive to this new state.

There are obvious differences between the present and earlier work. In general, the earlier data are in better absolute agreement with diffusion models.^{4,5,7} This may reflect the lower mobilities and to a limited extent, the lower fields available, but the situation is not yet clear. To look for systematic variations, more data are required on samples with a wider range of mobilities. If phonon drag proves to be essential in understanding the differences, then substrate properties are also fundamental to the behavior and should be characterized carefully. We have found the thermal conductivity to be a useful guide in this respect.

ACKNOWLEDGMENTS

We are grateful to Dr. A. R. Briggs of Centre National de la Recherche Scientifique (France) for suggesting the use of strain gauges as heaters. One of the authors (R.F.) would like to thank the Max Planck Institute for financial support while spending a year at Grenoble, the Natural Sciences and Engineering Research Council for a travel grant, and the many staff members at the Hochfeld-Magnetlabor who contributed to making the stay there very enjoyable.

*Permanent address: Physics Department, Queen's University, Kingston, Ontario, Canada K7L 3N6.

¹K. von Klitzing, G. Dorda, and M. Pepper, *Phys. Rev. Lett.* **45**, 494 (1980).

²D. C. Tsui, H. L. Stormer, and A. C. Gossard, *Phys. Rev. Lett.* **48**, 1562 (1982).

³H. Oji, *J. Phys. C* **17**, 3059 (1984).

⁴H. Obloh, K. von Klitzing, and K. Ploog, *Surf. Sci.* **142**, 236 (1984).

⁵H. Obloh, K. von Klitzing, K. Ploog, and G. Weimann, *Proceedings of the 13th Yamada Conference on the Electronic Properties of 2D Systems*, Kyoto, Japan, 1985 [*Surf. Sci.*].

- (to be published)].
- ⁶R. J. Nicholas, T. H. H. Vuong, M. A. Brummell, J. C. Portal, and M. Razeghi, in *Proceedings of the 17th International Conference on the Physics of Semiconductors, San Francisco (1984)*, edited by J. D. Shade and W. A. Harrison (Springer-Verlag, New York, 1985), p. 389.
- ⁷T. H. H. Vuong, R. J. Nicholas, M. A. Brummell, J. C. Portal, M. Razeghi, F. Alexandre, J. M. Masson, K. Y. Cheng, and A. Y. Cho, *Proceedings of the 13th Yamada Conference on the Electronic Properties of 2D Systems, Kyoto, Japan, 1985* [Surf. Sci. (to be published)].
- ⁸R. Fletcher, J. C. Mann, and G. Weimann, Phys. Rev. B **32**, 8477 (1985).
- ⁹M. Jonson and S. M. Girvin, Phys. Rev. **29**, 1939 (1984).
- ¹⁰H. Oji, Phys. Rev. **29**, 3148 (1984); J. Phys. C **17**, 3059 (1984).
- ¹¹W. Zawadzki and R. Lassnig, Surf. Sci. **142**, 225 (1984).
- ¹²P. Streda, Phys. Status Solidi B **125**, 849 (1984).
- ¹³R. J. Nicholas, J. Phys. C **18**, L695 (1985).
- ¹⁴C. Herring, Phys. Rev. **96**, 1163 (1954).
- ¹⁵G. A. Slack, Phys. Rev. **122**, 1451 (1961).
- ¹⁶R. Feder and T. Light, J. Appl. Phys. **39**, 4870 (1968).
- ¹⁷R. Herth and O. Weis, Z. Phys. **29**, 101 (1970).
- ¹⁸M. G. Holland, Phys. Rev. **132**, 2461 (1963); *ibid.* **134**, A471 (1964).
- ¹⁹J. M. Ziman, *Electrons and Phonons* (Oxford University Press, London, 1960), p. 465.
- ²⁰M. G. Holland, *Semiconductors and Semimetals*, edited by R. K. Willardson and A. C. Beer (Academic, New York, 1966), Vol. 2, p. 3.
- ²¹W. Walukiewicz, H. E. Ruda, J. Lagowski, and H. Gatos, Phys. Rev. B **30**, 4571 (1984); Phys. Rev. B **31**, 4034 (1985).
- ²²P. G. Klemens, Handb. Phys. **14**, 198 (1956).
- ²³B. J. Thaler and R. Fletcher, J. Low Temp. Phys. **30**, 773 (1978).